6

Great landslides

INTRODUCTION

(Moore, 1978; Lockridge, 1990; Masson, Kenyon, and Weaver, 1996; Dawson, 1999; Canals *et al.*, 2004)

The previous chapter on tsunamigenic earthquakes continually alluded to submarine landslides as being a contributing factor in the generation of anomalous tsunami. For example, the tsunami that swept Prince William Sound following the Great Alaskan Earthquake of 1964 and the one that swept the Pacific Ocean following the 1946 Alaskan earthquake are now recognized as being the products of submarine landslides. The latter event was large enough to affect Hawaii. Unfortunately, the evidence of sliding is difficult to obtain, especially in regions where detailed side-scan sonar surveys have not been performed beforehand.

About 70% of the Earth's surface consists of oceans containing tectonically and volcanically active areas near subduction zones. The oceans also consist of very steep topography along continental shelf margins, on the sides of ocean trenches, and on the myriad of oceanic volcanoes, seamounts, atolls, and guyots that blanket the ocean floor. Sediment moves under gravity down these slopes through a variety of processes that include slumps, slides, debris flows, grain flows, and turbidity currents. Debris flows can move without incorporating water; however, where material mixes with water, a dense turbid slurry of sediment can move as a current along the seabed under the effects of gravity. The latter are known as turbidity currents and form the distinct deposits that were described in Chapter 3. Substantial volumes of material are transported long distances, on slopes as low as 0.1°, across the deep ocean seabed by slides, flows, and turbidity currents. Slides consist of basal failure of topography that moves downslope in coherent blocks. As the slide progresses downslope it may disintegrate, producing a debris flow that mainly consists of disaggregated sediments.

Figure 6.1. Woodcut portraying the great flood of January 30, 1607 in the lowlands surrounding the Bristol Channel, U.K. Analysis of historical records and field evidence lends support for a tsunami as the cause of the flooding. A likely source would be a submarine slide off the continental shelf edge near Ireland. *Source:* White (1607).

Where large volumes of material are involved, these processes can generate tsunami ranging from small events concentrated landward of the failure to mega-tsunami an order of magnitude larger than those generated historically by earthquakes (Figure 6.1). The most notable event to occur in the 20th century was the Grand Banks tsunami of November 18, 1929. This event, to be discussed in detail subsequently, resulted from a slide that had a volume of 185 km^3. Geologically, larger slides with volumes over 5,000 km^3 are known. For example, debris flows around the Hawaiian Islands have involved these volumes, while the Agulhas slide off the South Africa coast contains a total of 20,000 km^3 of material (Table 6.1, Figure 6.2).

Landslides can take the form of slumping of rock and unconsolidated sediment, or rotation of material along planes of weakness in the rock. The latter often leaves a distinct scar or headwall eroded into the continental shelf slope or exposed on land as an amphitheater formed in cliff lines. Rotational slides may also generate transverse cracks across the body of the slipped mass and tensional cracks above the head scarp, which gives rise to subsequent failure. As shown in Chapter 5, earthquakes are the most likely triggering mechanism for landslides, especially submarine ones that have commonly been associated with tsunami. While terrestrial landslides falling into a body of water may be locally significant, this chapter will concentrate upon submarine landslides that have the potential to affect a much wider area of ocean.

Table 6.1. Area and volume of large submarine slides and their associated tsunami.

Location	*Area* (km^2)	*Volume* (km^2)	*Tsunami features*
Hawaiian Islands			
Nuuanu Slide	23,000	5,000	
Alika 1 and 2	4,000	600	May be responsible for the Lanai event, run-up >365 m
Storegga Slides, Norway	112,500	5,580	
First	52,000	3,880	
Second	88,000	2,470	
Third	6,000	Included in above	Maximum wave height of 5 m swept east coast of Scotland
Agulhas, South Africa	—	20,000	
Sunda Arc, Burma	3,940	960	
Saharan Slide	48,000	600	
Canary Islands	40,000	400–1,000	May be the cause of tsunami that swept the Bahamas (see Chapter 4)
Grand Banks, 1929	160,000	760	3 m high tsunami wave, Burin Peninsula, Newfoundland
Bulli, SE Australia	200	20?	May explain tsunami features in Sydney–Wollongong area

Source: Based on Moore (1978), Harbitz (1992), and Masson, Kenyon, and Weaver (1996).

CAUSES OF SUBMARINE LANDSLIDES

(Carlson, Karl, and Edwards, 1991; Masson, Kenyon, and Weaver, 1996; Bryant, 2005)

On dry land, slope failure can be modeled using the Mohr–Coulomb equation as follows:

$$\tau_s = c + (\sigma - \xi) \tan \varphi \tag{6.1}$$

where τ_s = the shear strength of the soil (kPa)
c = soil cohesion (kPa)
σ = the normal stress at right angles to the slope (kPa)
ξ = pore water pressure (kPa)
φ = the angle of internal friction or shearing resistance (degrees)

In this equation, pore water pressure is a crucial determinant in failure. Sediments that are water-saturated are more prone to failure, while factors that temporarily increase pore water pressure such as the passage of seismic waves can reduce the term $(\sigma - \xi)$ to zero. At this point, the strength of a soil becomes completely dependent

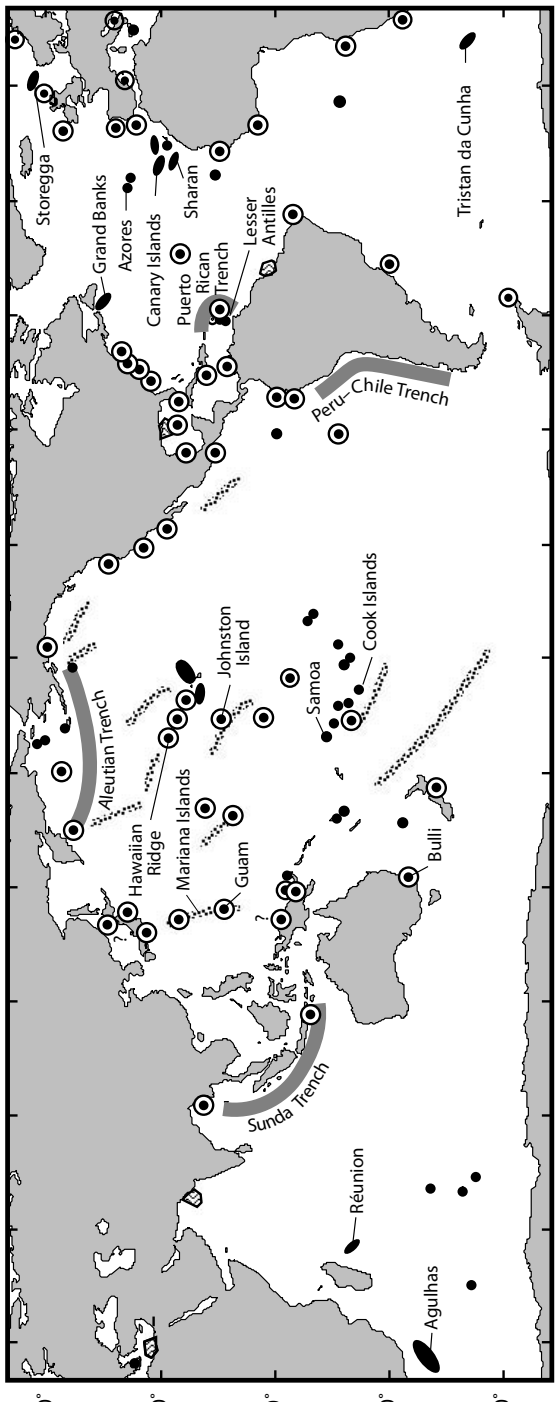

Figure 6.2. Location of major submarine slides and debris flows. Those parts of the oceans with topography susceptible to underwater landslides are also marked. Based on Moore (1978), Keating *et al.* (1987), Holcomb and Searle (1991), and Canals *et al.* (2004).

upon the cohesion within loose sediment or within stratified rocks. Material on submerged continental shelves and island flanks are water saturated and devoid of vegetation. Their slopes were drowned and became prone to failure because of a Holocene rise in sea level amounting to 100 m–130 m in the last 3,000–6,000 years. This resulted in an additional weight on the seabed of 103×10^6 t km^{-2}–133×10^6 t km^{-2}. Pore water pressure also increased internally within sediment lying at deeper depths with this rise in sea level. Slides in these environments usually occur close to the time of initial saturation. The Storegga Slides off Norway may be the best example of such a process.

Changes in sea level do not have to be large to induce failure. Storm surges associated with the passage of a tropical cyclone can load and deload the shelf substantially. For example, along the east coast of the United States, 7 m high surges are common. The resulting increase in weight on the seabed can be 7.2×10^6 t km^{-2}. If this is preceded by deloading due to the drop in air pressure as the cyclone approaches shore, then the total change in weight can amount to 10×10^6 t km^{-2}. In areas where the Earth's crust is already under strain, this pressure change may be sufficient to trigger an earthquake. The classic example of a cyclone-induced earthquake occurred during the Great Tokyo Earthquake of 1923. A typhoon swept through the Tokyo area on September 1 and was followed by an earthquake, a submarine slide, and an 11 m high tsunami that evening. In all, 143,000 people were killed. Measurements after the earthquake indicated that parts of Sagami Bay had deepened by 100 m–200 m with a maximum displacement of 400 m. These changes are indicative of submarine landsliding. In Central America, the coincidence of earthquakes and tropical cyclones has a higher probability of occurrence than the joint probability of both events. Finally, failures on the submerged front of the Mississippi Delta have occurred primarily during tropical cyclones.

The internal pressure within submerged sediment can also be increased by the formation of natural gas through anaerobic decay of organic matter that has accumulated through the deposition of terrestrially derived material. This process is known as under-consolidation and occurs when fluid pressure within sediments exceeds the hydrostatic pressure. Methane is also locked into sediment on lower slopes, but because of the near-freezing water temperature and the extreme pressure, it is preserved as a solid gas hydrate. If this hydrate decomposes back to methane, then either the increased pressure due to the release of the gas into the sediment or the formation of voids can cause failure.

Slopes of ongoing sediment accumulation can become overloaded and oversteepened, leading to failure. This was a major process on continental slopes during glacials when sea level was lower. The increase in grade and exposure of continental shelves to subaerial weathering permitted increased volumes of sediment to be emplaced on the shelf slope. The process dominated the terminal end of major river deltas. Slides in these environments consist of rotational slumps. In solid rock, cohesion may be low because of shear planes that exist along the bedding planes between sedimentary layers or by joints running through the rock. Stratigraphically favorable conditions for landslides include massive beds overlying weaker ones, alternating permeable and impermeable beds, or clay layers. Structurally favorable

conditions include steeply or moderately dipping foliations and cleavage, joint, fault, or bedding planes. Rock that is strongly fractured or jointed; or contains slickenside because of crushing, folding, faulting, earthquake shock, columnar cooling, or desiccation; is also likely to fail. Many rock units and sediment deposits on shelves thus have the potential for collapse.

Mid-ocean volcanic islands are particularly prone to large landslides. On average, four such failures have occurred on these types of islands each century over the past 500 years. Shield volcanoes over hot spots accrete through successive lava flows that solidify quickly when they contact seawater. The islands consequently can rise 4,000 m or more above the seabed as steep pedestals emplaced on poorly consolidated, deep ocean clays. If weathering occurs between flow events, then subsequent flows are deposited higher in the edifice over weaker strata that may become zones for failure. If a landslide occurs early in the building phase of a volcano, then its seaward-dipping surface and its cover of blocky debris can become an unstable, low-friction foundation for ensuing lava flows. Eruptive events may inflate the volcano, steepening bedding planes, and fracturing the dome-like structure. Fracture lines may become zones for dyke intrusion that can over-pressurize rock and increase its volume by more than 10%. For example, on the east side of Oahu, Hawaii, dykes make up 57% of the horizontal width of the shield volcano. In addition, the weight of edifices standing over 4,000 m high can cause crustal subsidence that fractures the volcano further. Many volcanoes contain rift zones extending throughout the edifice along these zones of weakness. The flanks of these volcanoes are being pushed sideways, over the top of the sediment layer at their base under the force of gravity or by magma injection. Rates of spreading range between 1 cm and 10 cm per year. For example, the southern flank of Kīlauea is presently moving at this higher rate away from a rift zone known as the Giant Crack. Giant landslides occur on the unbuttressed flanks of such volcanoes giving the volcano a tristar shape etched by steep headwall scars. This process is common on young volcanoes usually less than a million years in age, and has been a notable feature of the Hawaiian and Canary Islands.

HOW SUBMARINE LANDSLIDES GENERATE TSUNAMI

(Pelinovsky and Poplavsky, 1996; Watts, 1998)

The characteristics of tsunami generated by landslides are different from those simply generated by the displacement of the seabed by earthquakes. One of the more important differences is the fact that the direction of propagation of tsunami generated by landslides is more focused. The slide moves in a downslope direction, and the wave propagates both upslope and parallel to the slide. As a result, the tsunami wave has a shape that becomes exaggerated close to the source and is best characterized by an *N*-wave (Figure 2.4). The wave train is led by a very low-crested wave followed by a trough up to three times greater in amplitude. The second wave in the wave train has the same amplitude as the trough, but over time, it decays into three or four waves with decreasing wave periods. The initial inequality between the crest of the first wave

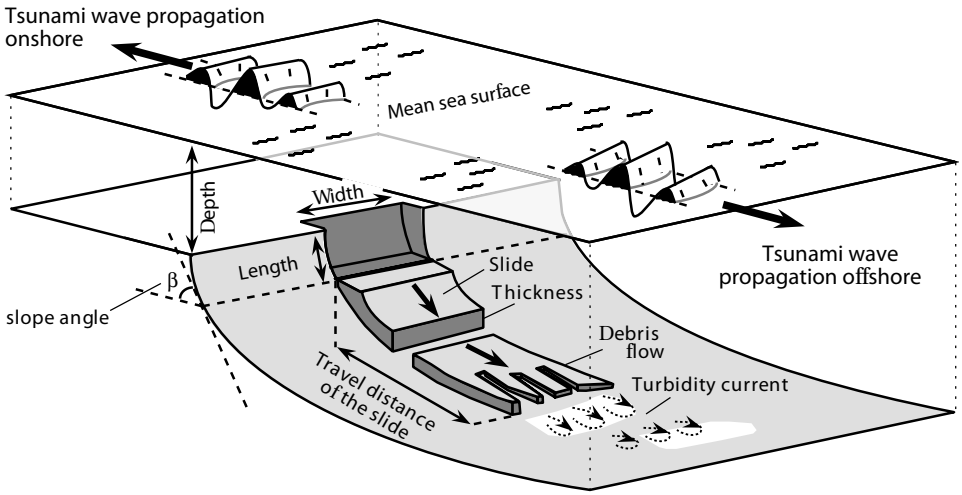

Figure 6.3. Schematic representation of a coherent submarine slide.

and the succeeding trough enables landslide-generated tsunami to obtain greater run-up heights than those induced by earthquakes.

Wave generation by landslides depends primarily upon the volume of material moved, the depth of submergence, and the speed of the landslide. The volume of material can be determined knowing the height of the slide, its horizontal length, and the initial slope (Figure 6.3). However, the characteristics of a slide critical to modeling tsunami are inevitably determined well after the event. The easiest slide to model is one where material fails as a coherent block. However, most slides disintegrate into a debris avalanche and eventually a turbidity current. Turbidity currents are irrelevant in the generation of tsunami, because by the time sediment has become mixed with water and begun to stratify in the water column, the tsunami has been generated and is moving away from its source area. Turbidity currents are only important in laying down distinct deposits that are more than likely a signature of paleo-tsunami.

Most slides slowly accelerate reaching a terminal velocity that depends upon the slide's mass and density, and the angle of the slope. Hence, a submarine landslide takes time to develop and generate any tsunami. If an earthquake triggers a tsunamigenic submarine landslide, the time between the earthquake and the arrival of the tsunami at shore is longer than expected. The wavelengths and periods of landslide-generated tsunami range between 1 km and 10 km and 1 min and 5 min, respectively. These values are much shorter than those produced by earthquakes. The wave period of a landslide-generated tsunami increases as the size of the slide increases and the slope decreases. It is independent of water depth, the depth of submergence, and the mass of the block. As a first approximation, the simplest slide to model is one that occurs on a slope of 45°. In this case, the maximum height of a tsunami wave above

still water can be approximated by the following formula:

$$H_{\max} \sim c^{1.75} d^{-0.75} \tag{6.2}$$

where c = the thickness of the slide (m)
d = the initial depth of submergence in the ocean (m)
$H_{\max}$ = the maximum height of a tsunami wave above still water

Submarine landslides rarely exceed $50\,\mathrm{m\,s^{-1}}$, while their associated tsunami travel at $100\,\mathrm{m\,s^{-1}}$–$200\,\mathrm{m\,s^{-1}}$. Recent modeling indicates that these latter velocities may approximate $1{,}500\,\mathrm{km\,h^{-1}}$. Hence, tsunami generated by submarine landslides outpace the slide that forms them and produces several simple long waves in a wave train. In this case, that maximum tsunami wave height becomes independent of bottom slope and the following equation may apply:

$$H_{\max} = 0.25\pi c^2 d^{-1} \tag{6.3}$$

These heights can be used to calculate other characteristics of the tsunami when it reaches shore using the equations presented in Chapter 2.

HISTORICAL TSUNAMI ATTRIBUTABLE TO LANDSLIDES

(Miller, 1960; Intergovernmental Oceanographic Commission, 1999)

Both terrestrial and submarine landslides can produce tsunami. While historically rare, both are impressive. For example, the largest tsunami run-up yet identified occurred at Lituya Bay, Alaska, on July 9, 1958 following a rockfall triggered by an earthquake. Water swept 524 m above sea level opposite the rockfall, and a 30 m to 50 m tsunami wave propagated down the bay toward the ocean. This tsunami will be described in detail subsequently. As pointed out in Chapter 1, steep-sided fjords in both Alaska and Norway are also subject to slides. There have been seven tsunamigenic events in Norway, which together have killed 210 people. The heights of these tsunami ranged between 5 m and 15 m with run-ups of 70 m above sea level close to the source. Five of these events occurred in Tafjord in 1718, 1755, 1805, 1868, and 1934. In the April 7, 1934 event, $1 \times 10^6\,\mathrm{m^3}$ of rock dropped 730 m from an overhang into the fjord. The initial tsunami was 30 m–60 m high, decaying to 10 m several kilometers away. It traveled at a velocity of $22\,\mathrm{km\,h^{-1}}$–$43\,\mathrm{km\,h^{-1}}$. Historically, a slide 16 times this volume has occurred in Tafjord. Loen Lake in Norway has also been subject to slide-induced tsunami, with three events occurring in 1936 alone. The largest of these produced run-ups of 70 m above lake level, killing 73 people. In the United States, slides have also generated tsunami in Disenchantment Bay, Alaska on July 4, 1905, and several times in Lake Roosevelt, Washington. The Disenchantment Bay event produced maximum run-up of 35 m, 4 km from the source, while slides into Roosevelt Lake have generated run-ups of 20 m on at least two occasions. One of the more unusual tsunami produced by a rockslide occurred in the Vaiont Reservoir in Italy in October 1963. Here, $0.25 \times 10^9\,\mathrm{m^3}$ of soil and rock fell into the reservoir sending a wave 100 m high over the top of the dam and down the valley, killing 3,000

people. Even small earthquakes can generate tsunamigenic submarine landslides, sometimes hours after the event. The Kona earthquake of 1951 in Hawaii had a magnitude of only 6.7; yet, it produced a tsunami with a maximum run-up of 1.5 m as the result of a landslide that occurred three hours afterwards.

Tsunami generated by submarine slides have been common historical occurrences. For example, the Grand Banks earthquake of November 18, 1929 triggered a submarine landslide that is famous for the turbidity current that swept downslope into the abyssal plain of the North Atlantic. Less well known is the devastating tsunami that swept into the Newfoundland coast. Similarly, the 11 m high tsunami that swept the foreshores of Sagami Bay after the Great Tokyo Earthquake of September 1, 1923 is now thought to have been produced by submarine landslides. Major tsunami generated by submarine slides triggered by earthquakes have also occurred at Port Royal, Jamaica, in June 1692; at Ishigaki Island, Japan, on April 4, 1771; and at Seward, Valdez, and Whittier, Alaska, following the Great Alaskan Earthquake of 1964. The Port Royal tsunami flung ships standing in the harbor inland over two-story buildings and killed 2,000 inhabitants, while the Ishigaki Island tsunami carried coral 85 m above sea level and killed 13,486 people. The Sanriku tsunami of 1933, which took 2,144 lives, may also have been the product of a submarine slide triggered by an earthquake because a submarine canyon lying offshore was deepened by 590 m.

In the Pacific region alone, there have been 16 tsunami events since 1770, in which submarine landslides were triggered by earthquakes, killing 68,832 people. Since 1596, another 65 tsunami events involving either submerged or terrestrial landslides took a further 14,661 lives. Together, landslide-induced tsunami may have been involved in 12% of all deaths due to tsunami in the Pacific Ocean region. In the 20th century, submarine slides have occurred off the Magdalena River, Colombia, and the Esmeraldas River, Ecuador, in the Orkdals Fjord, and off several Californian submarine canyons. In 1953, submarine landslides cut cables in Samoa and produced a 2 m high tsunami. On July 18, 1979, a tsunami generated by a landslide, unaccompanied by any earthquake or adverse weather, destroyed two villages on the southeast coast of Lomblen Island, Indonesia, killing at least 539 people. Smaller tsunami were produced by submarine slides at Nice, France, on October 16, 1979; at Kitimat Inlet, British Columbia, on April 27, 1975; and in Skagway Harbor, Alaska, in November 1994. In the latter two cases, run-ups of 8.2 m and 11 m, respectively, were observed.

The Lituya Bay landslide of July 9, 1958

(Miller, 1960; Pararas-Carayannis, 1999)

Lituya Bay is a T-shaped, glacially carved valley lying entirely on the Pacific Plate. Glaciers reach almost to sea level in Crillon and Gilbert Inlets at the head of the Bay (Figure 6.4). The main bay measures 11.3 km long and 3 km wide, with a 220 m maximum depth. Cenotaph Island obstructs the center of the bay, and La Chaussee Spit, which is the remnant of an arcuate terminal moraine left over from the last glaciation, blocks the entrance to the sea. The bay has been subject to giant waves

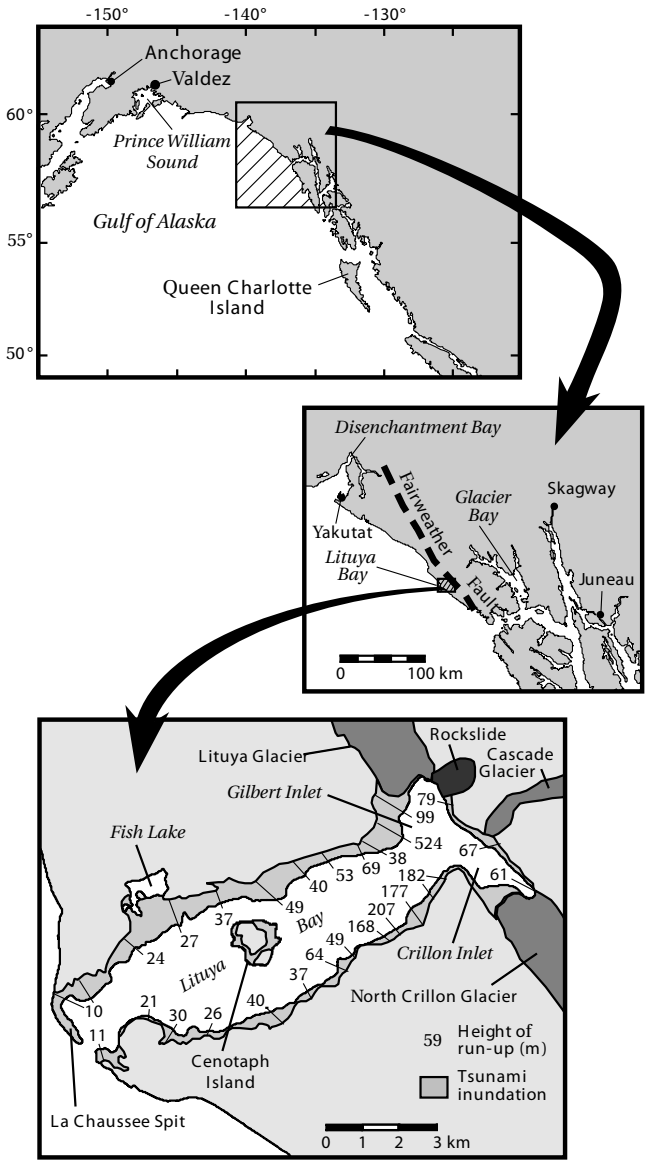

Figure 6.4. Location map of Lituya Bay, Alaska.

geologically. For example, run-ups of 120 m and 150 m above sea level were produced by events in 1853 and on October 27, 1936, respectively. The July 9, 1958 event is the largest, however, reaching an elevation of 524 m above sea level. The trigger for the event was an earthquake with a magnitude, M_s, of between 7.9 and 8.3 that occurred around 10:16 PM along the Fairweather Fault at the junction of the Pacific and North

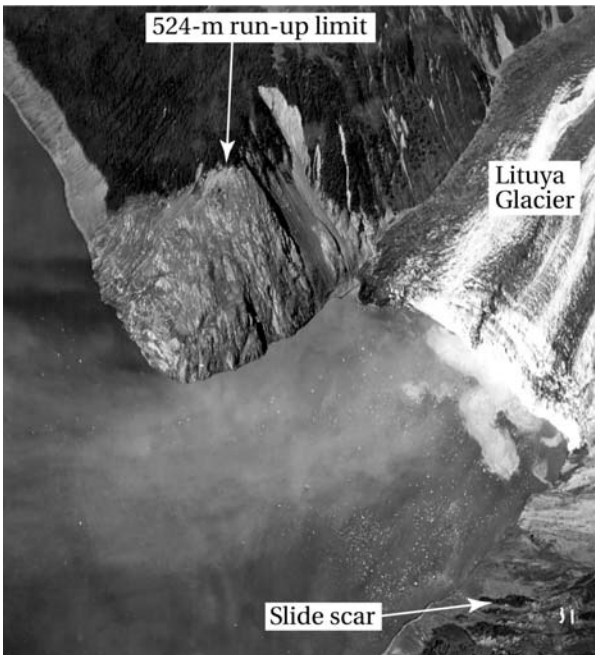

Figure 6.5. Site of the 524 m high run-up produced by the wave in Lituya Bay. *Source: http://libraryphoto.cr.usgs.gov/htmllib/btch229/btch229j/btch229z/mdj01289.jpg*

American Plates. The earthquake's epicenter was 20.8 km southeast of the head of Lituya Bay. Vertical and horizontal ground displacements of 1.1 m and 6.3 m, respectively, occurred along the fault and reached the surface in Crillon and Gilbert Inlets at the head of Lituya Bay. Vertical and horizontal accelerations reached 0.75g and 2.0g, respectively, in the region. None of these disruptions was sufficient to generate a giant wave. The earthquake triggered landslides in the northern part of the embayment. Terrestrial landslides are inefficient mechanisms for tsunami generation because only about 4% of their energy goes into forming waves. No known landslide has ever produced a wave the size of the Lituya Bay wave, which reached eight times the height above sea level of the largest slide-generated wave recorded in any Norwegian fjord. A Jökulhlaup or water bursting from an ice-dammed lake high up on Lituya Glacier could have also caused the wave. The water level in this lake dropped 30 m following the earthquake, and the hydraulic head was certainly sufficient to generate a giant wave. However, neither the volume of water nor the rate at which the lake drained was sufficient to allow such a high wave to develop. Besides, the maximum wave run-up did not occur near the discharge point for any Jökulhlaups or glacier burst from the glacier.

The tsunami appears to have been created by a sudden impulsive rockfall. Within 50 to 60 seconds of the earthquake, $30.5 \times 10^6\,m^3$ of consolidated rock dropped 600 m–900 m from the precipitous northeast shoreline of Gilbert Inlet into the bay (Figure 6.5). The impact of this rockfall was analogous to that of a meteoroid

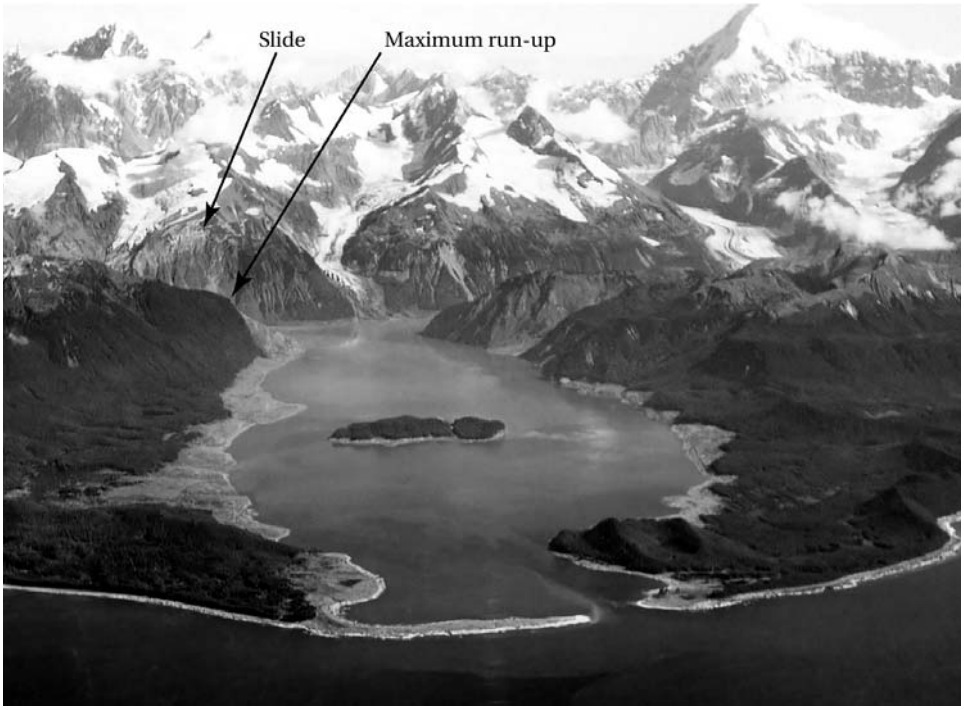

Figure 6.6. Aerial photograph of the foreshores of Lituya Bay swept by the tsunami of July 9, 1958. *Source: http://libraryphoto.cr.usgs.gov/htmllib/btch132/btch132j/btch132z/mdj01278.jpg*

crashing into an ocean—a phenomenon that will be described in Chapter 8. The impact not only displaced an equivalent volume of water, it also created a large radial crater in the bottom sediments of the lake that left an arcuate ridge up to 250 m from the shoreline. The sudden displacement of water and sediment sheared 400 m off the front of Lituya Glacier and flung it high enough into the air that a distant observer reported seeing the glacier lift above a ridge that had hidden it from view. On the opposite spur to the glacier, splash from the impact swept upslope to a height of 524 m above sea level, or more than three times the water depth of Gilbert Inlet. This splash has been mistaken for a giant wave of solid water; however, it probably entrained a considerable volume or air. The rockfall, in combination with ground uplift at the head of the bay, generated a solitary wave 30 m high that swept down the bay to the ocean at a speed of 155 km h^{-1}–210 km h^{-1}. Mathematical modeling using the same incompressible, shallow-water long-wave equations described in Chapter 2 supports these figures. Run-up from the wave swamped an area of 10.4 km^2 on either side of the bay and penetrated as much as 1 km inland (Figure 6.6). Soil and glacial debris were swept away, exposing clean bedrock; however, little erosion of bedrock took place despite theoretical water velocities as high as 30 m s^{-1}.

Grand Banks tsunami, November 18, 1929

(Heezen and Ewing, 1952; Long, Smith, and Dawson, 1989; Whelan, 1994; Dawson *et al.*, 1996; Piper, Cochonat, and Morrison, 1999)

The Grand Banks tsunami was produced by a submarine landslide or slump triggered at 5:02 PM by an earthquake that had a surface wave magnitude, M_s, of 7.2. The earthquake had an epicenter in about 2,000 m depth of water (Figure 6.7). Numerous submarine slides occurred in a 120 km to 260 km wide swathe over a distance of 110 km along the slopes of the continental shelf. The slides occurred at two scales, as small rotational slumps 2 m–5 m thick and as larger ones 5 m–30 m thick. These coalesced over several hours into debris flows and then a turbidity current. The event is noteworthy because it was the first submarine debris flow detected. The turbidity current was hundreds of meters thick and swept downslope over the next 11 hours, cutting 12 telephone cables between Europe and North America. Based upon the time when each cable was broken, the turbidity current obtained a maximum velocity of $15\,m\,s^{-1}$–$20\,m\,s^{-1}$. At its terminus, the resulting turbidite covered an area of $160{,}000\,km^2$ of seabed with $185\,km^3$ of sediment, to a maximum depth of 3 m. Sediment was deposited more than 400 km from the site of the slump in water depths of more than 2,500 m. This is one of the biggest turbidity currents yet identified either historically or geologically.

Little publicity has been given to the tsunami that followed the 1929 event. Two and a half hours after the earthquake, a 3 m high wave surged into the Burin Peninsula on the south coast of Newfoundland, directly opposite the headwall of the slide (Figure 6.7). The wave was caused by backfilling of the depression left in the ocean by the removal of material that formed the turbidity current. It is difficult to attribute the wave to a single rotational slide because hundreds were involved. However, a cluster of large slides occurred in 600 m depth of water directly south of the Burin Peninsula. The wave traveled at a velocity of $140\,km\,h^{-1}$ and was concentrated by refraction into the coves along this coast, where 40 isolated fishing communities were sheltered. The story in Chapter 1 refers to this wave as sheep riding a rising mountain of water in the moonlight (Figure 1.1). The tsunami wave train reached the coast on top of a high spring tide and surged up the steep shores as three successive waves, destroying boats and houses and carrying sediment into small coastal lagoons. The characteristic tsunami signature of a fining-upward sand layer, sandwiched between peats, has been identified in the lagoons at Taylors Bay and Lamaline. Run-up varied between 2 m and 7 m with an extreme value of 13 m elevation at St. Lawrence. Two other waves in rapid succession followed the first wave. Twenty-eight people died in Newfoundland. So isolated were the communities that news of the disaster did not reach the outside world until two days later. The tsunami was not restricted to Newfoundland. The wave also radiated out from the headwall of the slide and swept down the coast of Nova Scotia, fortunately without killing anybody. Fortunately, by the time it reached Halifax, the wave was only 0.5 m high. The wave also spread throughout the North Atlantic Ocean and was measured on tide gauges as far away as South Carolina and Portugal, although no damage was reported.

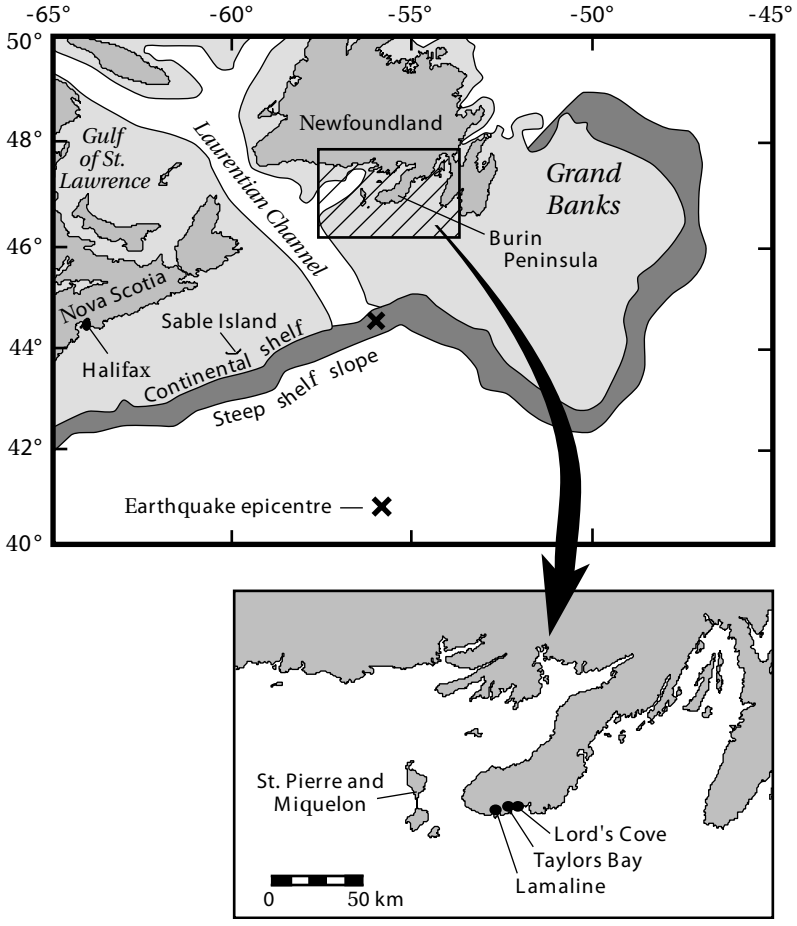

Figure 6.7. Location of the Grand Banks earthquake of November 18, 1929 and the Burin Peninsula of Newfoundland affected by the resulting tsunami.

The event is considered rare for this part of the North American coast, with a recurrence interval of 1,000–35,000 years. However, a similar, but smaller, event occurred in the same region in 1884. This tsunami was also triggered by an earthquake and submarine cables were broken. Since European settlement in North America, three other large earthquakes along the east coast could have generated tsunami if they had happened at sea or triggered submarine landslides. These events occurred at Cape Anne, Massachusetts, in 1755; Charleston, South Carolina, in 1886; and Baffin Bay in 1934. While rare, the Grand Banks Slide illustrates that the east coast of North America is susceptible to deadly tsunami caused by slides. Large submarine slides are a common bathymetric feature of the eastern continental margin of North America and the Gulf of Mexico, and will occur again.

GEOLOGICAL EVENTS

Hawaiian landslides

(Lipman *et al*., 1988; Moore and Moore, 1988; Moore, Bryan, and Ludwig, 1994; Moore, Normark, and Holcomb, 1994; Masson, Kenyon, and Weaver, 1996)

Some of the best evidence for giant submarine landslides has been discovered on the Hawaiian Islands using GLORIA (Geologic Long-Range Inclined Asdic), SeaBeam, and HMR-1 wide-swathe, side-scanning sonar systems. These systems sweep a swathe 25 km–30 km wide and measure features on the seabed down to 50 m in size. At least 68 major landslides more than 20 km long have been mapped over a 2,200 km length of the Hawaiian Ridge, between the main island of Hawaii in the southeast and Midway Island in the northwest (Figure 6.8). The average interval between events is estimated to be 350,000 years. Because shield volcanoes typically have triple-junction rift zones, amphitheaters are cut into the volcano at the headwall of giant landslides.

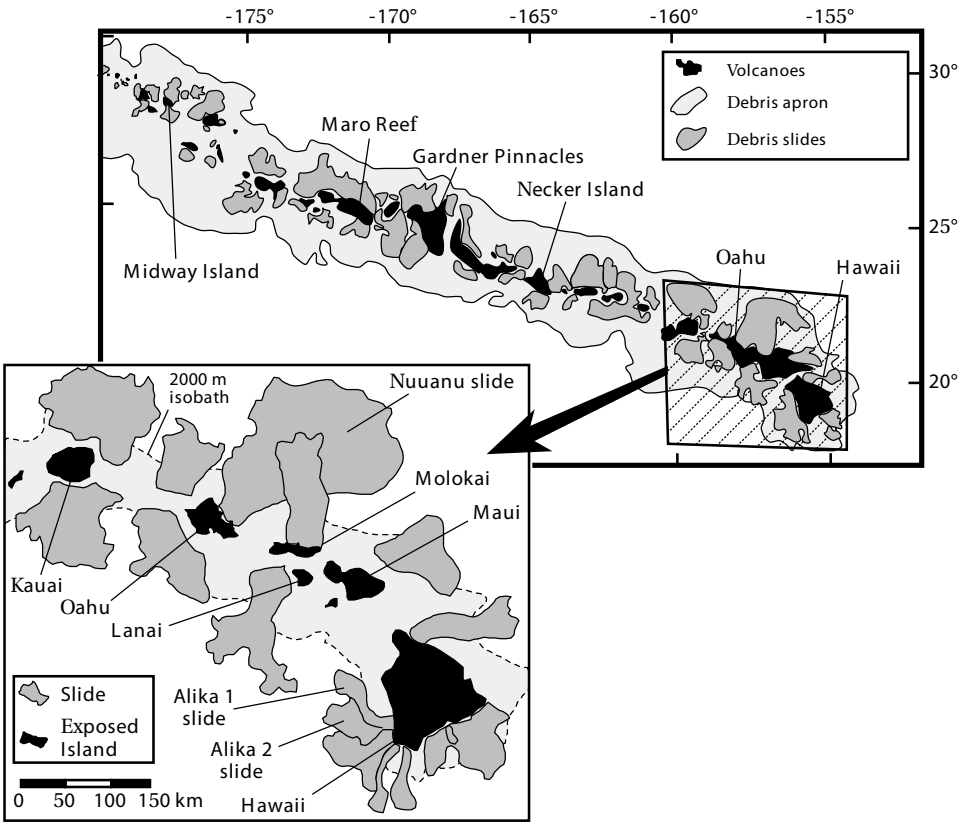

Figure 6.8. Location of submarine slumps and debris flows on the Hawaiian Ridge. Based on Moore *et al*. (1989), and Moore, Normark, and Holcomb (1994).

If landslides have been ubiquitous on an island, then the island takes on a stellate shape termed a Mercedes star. On older volcanoes, these head scarps may be buried by subsequent volcanic activity. Some of the largest landslides occurred near the end of shield building when a volcano stood 2 km–4 km above sea level. The major trigger for the avalanches was earthquakes on the younger islands; however, on the older islands mass failures are even triggered by storm surges and internal waves. The length of the slides increases from 50 km to 100 km for the older western volcanoes to 150 km–300 km for the younger eastern ones—making them some of the longest slides on Earth. The volume of material in each slide is as much as 5,000 km^3. Smaller landslides having volumes of tens of cubic kilometers have also been detected in shallower waters but not mapped in detail because of the difficulty of using side-scan sonar at these depths. In total, about half of the volume of the Hawaiian Ridge consists of landslide material. The landslides can be grouped into slower moving slumps and faster moving debris flows. The latter have the potential for generating colossal tsunami wave heights.

Slumps have an internal consistency whereby large chunks slough off from a volcano along fault lines or rifting zones to a depth of 10 km. Parts of slumps may produce smaller debris avalanches. Slumps and their resulting tsunami are historically common in Hawaii. In 1868, slumps associated with an earthquake with a recorded magnitude, M_s, of 7.5, produced a 20 m high tsunami that killed 81 people. In 1919, a similar magnitude earthquake produced a submarine landslide off Kono that resulted in a 5 m high tsunami run-up. In 1951, a small earthquake generated a local tsunami at Napoopoo. Two hours later, part of a cliff fell into Lealakakua Bay and generated another local tsunami. In 1975, an earthquake again with a recorded magnitude, M_s, of 7.5 caused a 60 km section of the flank on Kīlauea to subside 3.5 m and to move 8 m into the ocean. The resulting tsunami had a maximum run-up height of 14.3 m, killing two people.

Submarine debris avalanches are morphologically similar to those witnessed on volcanoes on land where speeds of several hundred kilometers per hour have been inferred. If the Hawaiian debris avalanches obtained similar velocities, then they were major agents for tsunami generation in the Pacific. Unlike slumps, debris avalanches are thinner, having thicknesses of 0.05 m–2.0 m; however, they may travel as far as 230 km on slopes as little as 3°. The largest submarine avalanche is the Nuuanu debris avalanche on the northern side of Oahu Island (Figure 6.8). It is 230 km long, with a maximum thickness of 2 km at its source. It covers an area of 23,000 km^2 and has a volume of 5,000 km^3 (Table 6.1). This represents one of the largest debris avalanches on Earth. It possibly occurred 200,000 years ago and would have sent a wave 20 m high crashing into the United States west coast. Debris avalanches are characterized by hummocky terrain at their distal end with some of the hummocks consisting of blocks of volcanic rock measuring 1 km–10 km in width. The largest individual block identified so far occurs in the Nuuanu deposit and measures 30 km × 17 km × 1.5 km.

The Alika debris avalanches on the western side of the main island of Hawaii are two of the youngest events in the island chain (Figure 6.8). The older avalanche, Alika 1, covers an area of 2,300 km^2; the younger, Alika 2, is slightly smaller, covering an area of 1,700 km^2. Together, both failures incorporate 600 km^3 of material,

although the volume of material missing from the western side of Hawaii Island totals 1,500 km^3–2,000 km^3—much of it originating underwater down to 4,500 m depths. The second slide traveled more than 50 km from the coast in a northwesterly direction toward the small island of Lanai. Uncharacteristically steep slopes, reaching 2,000 m above sea level on the southwest side of Mauna Loa, appear to represent the headwall of the slides. Failure occurred in the unbuttressed flanks of Mauna Loa and Hualalai volcanoes along rift zones infilled with dykes. Sedimentation rates on these slide deposits suggest that they are only a few hundred thousand years old. This age and the potential of the slides for tsunami generation link them to anomalously high beach deposits of a similar age on nearby islands.

Evidence that the Alika slides generated a major tsunami comes from gravel and boulder beds found on nearby islands to the northwest. These deposits reach elevations above sea level of 61 m on the southeastern tip of Oahu, 65 m on the south coast of Molokai, 73 m on the west coast of Maui, 79 m on the northwest corner of Hawaii, and 326 m on the south coast of Lanai. On Lanai, catastrophic wave run-up may have deposited discontinuous dune-like boulder ridges, known as the Hulopoe Gravel, up gullies and on interfluves. The waves were also erosive removing a 2 m depth of weathered soil and basalt in a 2 km wide strip parallel to the coast. The highest elevation of stripping is 365 m above sea level on Lanai and 240 m on the west side of Kahoolawe. On the northeast sides of both islands, the height of stripping only reached 100 m above sea level. Because all islands are rising, the elevation of run-up would have been lower than these values at the time of the tsunami.

This stripping removed spherically weathered basaltic boulders up to 0.5 m in diameter from the soil and swept then downslope. These boulders were then re-entrained by subsequent waves, together with coral gravel, and deposited in three inversely graded beds up to 4 m thick. The size of boulders and thickness of the deposit decreases upslope to a 150 m elevation. The larger particles support each other and are imbricated upslope—facts indicative of transport in suspension or as bedload. The voids between the large clasts are infilled with silt and pebbles that include marine foraminifera and sea-urchin spines. Fine calcareous material can be found filling crevices to an altitude of 326 m on Lanai. Mollusk shells are scattered throughout the deposit with species derived from 20 m to 80 m depths of water characteristic of a slightly warmer environment than exists at present. The surface of the deposit consists of a branching network of ridges with a relief of 1 m and a spacing of 10 m. The ridges are asymmetric in profile with the steepest end facing downslope—a fact suggesting that backwash was the last process to mould the surface.

The hydrodynamics of the flow can be determined from this internal fabric and morphology. The inverse grading is suggestive of a thin, fast-moving sheet of water typical of wave run-up or backwash. With a dune spacing of 10 m and a maximum boulder size of 1.5 m, the flow of water was 1.6 m deep—Equation (3.4)—and obtained a minimum velocity of 6.3 $m\,s^{-1}$—Equation (3.1). These conditions are favorable for deposition of inversely graded deposits under run-up or backwash. The boulder-sized material and high elevation of deposition and stripping indicate that the flow velocity and run-up limits were an order of magnitude greater than that

produced by storm waves or by tsunami generated by a distant tectonic event. The latter have a recorded maximum run-up height of no more than 17 m on these islands. The presence of multiple beds indicates a wave train that included three or four catastrophic waves, with the second wave being most energetic and reaching a maximum elevation of 365 m above sea level. If run-up height is set at ten times the tsunami wave height approaching shore, then the tsunami wave was 19 m–32 m high when it reached the coast. This is a conservative estimate, given the steep slopes of the islands and the fact that the swash was sediment laden. Only waves generated by submarine landslides or asteroid impacts with the ocean are this big. The first wave in the tsunami wave train picked up material from the ocean, washed over and dissected any offshore reefs, and carried all this material in suspension, at high velocity, up the slopes of the islands. The first wave was so powerful on Molokai that it cracked the underlying bedrock to a depth of 10 m. These crevices were then subsequently infilled with fluidized sediment. The first wave also picked up boulders from the weathered surface as it swept upslope. These were then mixed with the marine debris in the backwash and laid down by subsequent waves into graded beds. The last backwash molded the surface of the deposits into dune bedforms.

The asymmetry in the elevation of maximum stripping around Lanai and Kahoolawe suggests that the source of the tsunami had to be from the southeast. Uranium–thorium dates from the coral on Lanai show that the event occurred during the Last Interglacial around 105,000 years ago. However, the deposit on Molokai represents an older event that occurred at the peak of the Penultimate Interglacial 200,000–240,000 years ago. The most likely source of the tsunami was one or more of the Alika submarine debris avalanches off the west coast of the main island of Hawaii. Slides to the southwest of Lanai cannot be ruled out, but they are older than the age of the deposits. If this latter source caused the tsunami, then the wave must have been generated by water backfilling the depression left in the ocean. This mechanism is similar to that proposed for the tsunami that swept the Burin Peninsula on November 18, 1929. The tsunami could also have been generated by an asteroid impact in the Pacific Ocean off the southeast coast of Hawaii. Asteroids as agents of tsunami generation will be discussed in Chapter 8. Unfortunately, the Hulopoe Gravel on Lanai has been questioned as a tsunami deposit. Some locations covered in Hulopoe Gravel also contain soil profiles between layers, and it is difficult to envisage deposition up gullies that should have then been scoured by backwash. Finally, the imprint of human activity cannot be ignored in the deposition of either some of the boulder piles or mollusks on Lanai.

The Canary Islands

(Masson, 1996; Carracedo *et al.*, 1998)

The Canary Islands have formed over the last 20 million years as shield volcanoes that rise from depths of 3,000 m–4,000 m in the ocean to heights of 1,000 m above sea level. The islands are similar to the Hawaiian Islands in that their origin has been linked to hot-spot activity. Because of structural control and scarring by 14 landslides, the islands have taken on Mercedes star outlines (Figure 6.9). The

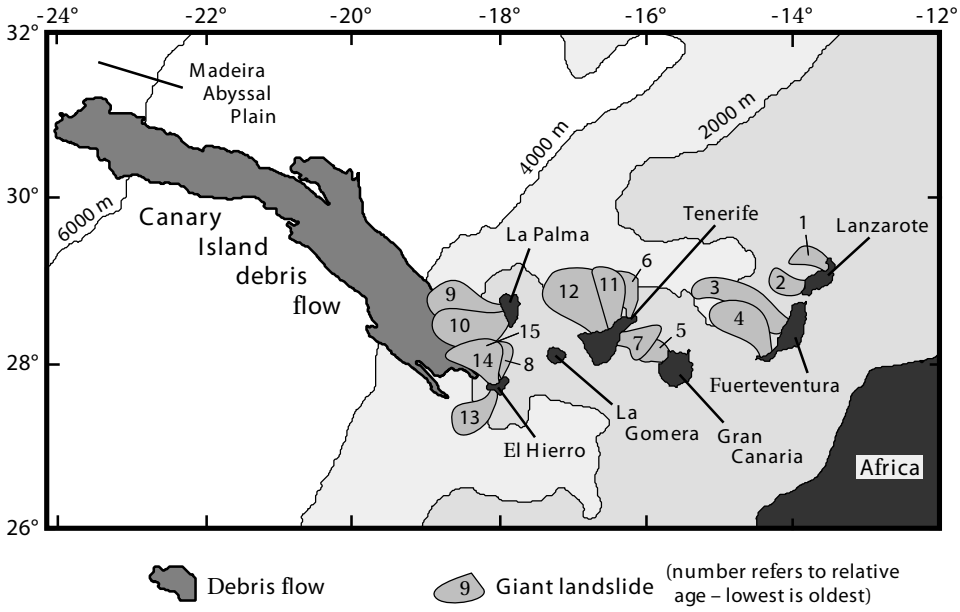

Figure 6.9. The giant landslides of the Canary Islands. Based on Masson (1996), and Carracedo *et al.* (1998). The debris flows are numbered sequentially according to decreasing age.

scars consist of large amphitheaters or depressions that are backed by high cliffs. The most prominent of these lie on the island of El Hierro where landslides have left a Matterhorn-like peak. As well, there are two prominent scars on Tenerife to the east. Giant landslides occur more frequently on the younger islands that are less than 2 million years old. Seven turbidites, ranging in volume from 5 km^3 to 125 km^3 and linked geochemically to the islands, have been mapped on the abyssal plain west of the Canary Islands. All are less than 650,000 years old. The slides associated with these turbidites reach volumes of 1,000 m^3 and were most likely induced by over-steepening of the volcanoes through successive eruptions or by the emplacement of vertical dykes.

Most of the debris flows have formed on the west side of the islands. Two of the oldest occur on the west sides of El Hierro and La Palma Islands, and are more than 550,000 years old. The largest debris flow on Tenerife Island occurred as recently as 170,000 years ago. El Hierro—the youngest island—has undergone the most recent activity. Two slides exist on the northwest corner of El Hierro. The older slide is 133,000 years old and has been proposed as a possible source for the tsunami that deposited chevron ridges on the Bahamas during the Last Interglacial. The younger slide contains by far the largest mass of debris identified as originating from the Canary Islands. Its headwall scarp is at least 8 km long and up to 900 m high. A debris avalanche, deposited closest to shore, contains individual blocks 1.2 km in diameter and 200 m high. Farther seaward, a debris flow 50 m–75 m thick was laid down. It is known as the Canary Island debris flow and covers an area of 1,500 km^3 (Figure 6.9).

This debris flow merges into a turbidite that is spread out on the seabed 600 km to the west of the islands. All the deposits are linked to a single catastrophic failure, involving 700 km^3–800 km^3 of material that occurred 13,000–17,000 years ago when global sea levels were over 100 m lower than present.

Tsunami deposits have now been identified in the Canary Islands and linked by their juxtaposition to landslides on Tenerife. None has been dated, however, so they cannot be associated with any specific debris avalanche. One deposit has been mapped on the Jandía Peninsula on the south side of Fuerteventura Island. The deposit is unstratified and consists of well-rounded boulders and pebbles, marine mollusks, and angular pieces of basalt. It lies at an elevation of 35 m–75 m above present sea level up to 1 km inland. Fuerteventura Island is tectonically stable, so the elevation of the deposit cannot be attributed to tectonic uplift. A similar deposit, consisting of two upward-coarsening beds of beach boulders and shell, has also been discovered up to 90 m above present sea level at Agaete, on the northwest coast of Gran Canaria. A deposit containing shell also exists more than 200 m above sea level on La Palma.

The Storegga slide of 7950 BP

(Hall, 1812; Long, Smith, and Dawson, 1989; Harbitz, 1992; Henry and Murty, 1992; Dawson, 1994; Bondevik, Svendsen, and Mangerud, 1997; Bondevik *et al.*, 1997; Canals *et al.*, 2004)

In 1815, Sir James Hall postulated that a range of bedrock-sculpturing features that included hairpin erosion marks several meters in length and the crag-and-tail hills that make up the city of Edinburgh were shaped by a tsunami similar to the one that had destroyed Lisbon in 1755. It was one of the first attempts in geology to explain the evolution of a landscape by invoking a single physical process. Hall of course was wrong. He knew nothing about continental glaciation that was subsequently used to explain the landforms. He was also unfortunate in picking the wrong landforms as examples. Had he examined the raised estuary plains (carseland) or the rocky headlands that dominate the east coast of Scotland, he would have found not only his signatures for catastrophic tsunami, but also many of the additional ones presented in Chapter 3. The tsunami did not originate in the North Atlantic as Hall envisaged, but from the region of known submarine slides at Storegga off the east coast of Norway (Figure 6.10). While not large enough to swamp the hills of Edinburgh, they were certainly a significant factor in molding the coastal landscape of eastern Scotland.

There have been five Storegga (great edge) slides in the past 30,000 years involving 5,580 km^3 of sediment that collapsed along 290 km of the continental slope of Norway. These slides sit on a series of much older ones stacked up on the seabed over the past half million years. The recent slides traveled over 500 km across the seafloor at velocities up to 50 $m\,s^{-1}$ (Figure 6.10). The average thickness of the resulting deposits is 88 m, with values as high as 450 m. The slides contain blocks measuring 10 km × 30 km that are up to 200 m thick. Sediment moved into water more than 2,700 m deep and formed turbidity currents over 20 m thick. This thickness is seven times more than that of the turbidite deposited by the Grand Banks Slide of

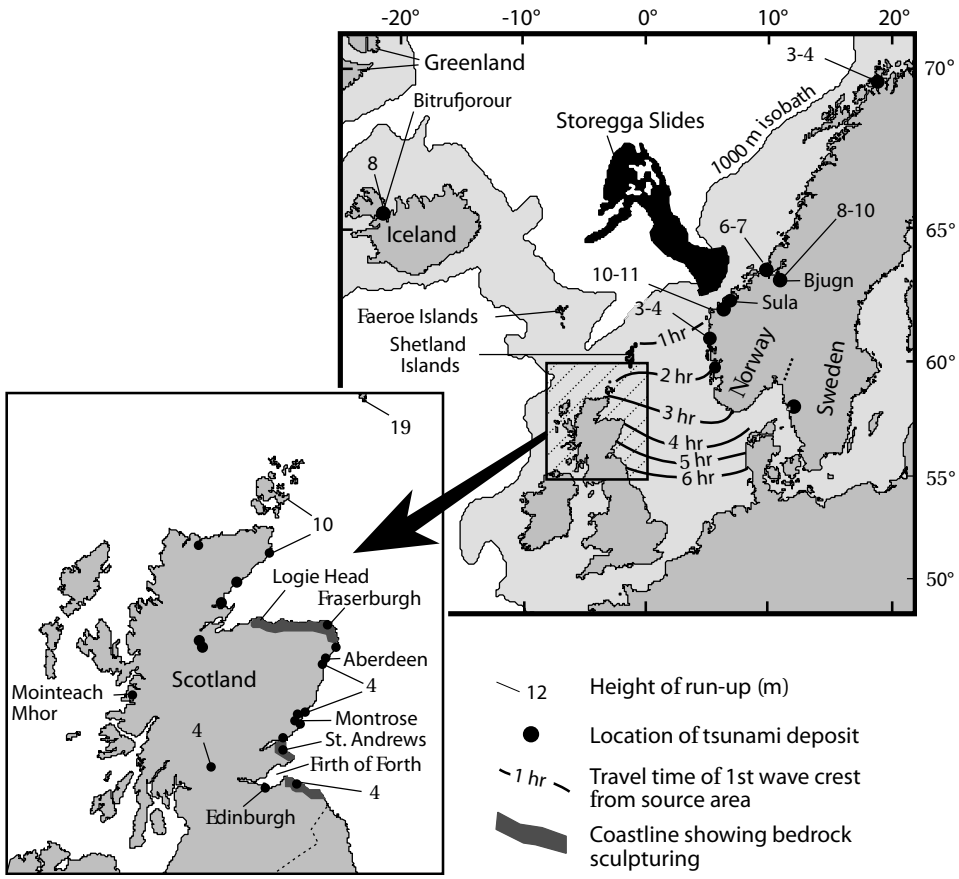

Figure 6.10. Location of the Storegga slides near Norway and coastlines in the North Atlantic affected by the resulting tsunami from the second event. Run-ups based on Dawson (1994), and Bondevik, Svendsen, and Mangerud (1997). Travel times in the North Sea are from Henry and Murty (1992).

November 18, 1929. The triggering mechanism for the Storegga slides is uncertain, but earthquakes and decomposition of gas hydrates within sediments have been suggested as causes.

The first slide occurred over 30,000 years ago, while the last two occurred close together between 6,000 and 8,000 years ago. The first slide was the biggest, involving 3,880 km^3 of sediment; however, any tsunami that it generated happened at lower sea levels and had little visible effect on today's coastline. The last two slides moved or remobilized 1,700 km^3 of sediment. Most of the evidence for catastrophic tsunami comes from the second Storegga slide, which has been radiocarbon-dated as being $7{,}950 \pm 190$ years old. The modeled deep-water wave height of the tsunami was 8 m – 12 m at its source and 2 m–3 m where it swept into the North Sea and the open Atlantic Ocean. Equation (6.2) yields a tsunami height of 2.3 m in the open ocean

based upon the geometry of the slide. The tsunami had a wave period of two to three hours—values that are much longer than those normally associated with earthquake-induced tsunami. The first wave reached the northeast coasts of Iceland and Scotland in just over two hours and took another eight hours to propagate through the North Sea (Figure 6.10). Most of the tsunami's energy was focused toward Greenland and Iceland. Based on shallow-water long-wave equations, the tsunami was 3 m high approaching the coast of Greenland and Iceland, and 1 m high approaching Scotland. Maximum run-up heights were 10 m–15 m for the first slide and 5 m–8 m for the second. Along the east coast of Scotland, modeled run-ups ranged from 3.0 m to 5.5 m. These values may be conservative. If the slide moved at a maximum theorized velocity of 50 m s^{-1} or initially underwent rapid acceleration, then the calculated run-up heights of the second slide were 13.7 m along the east coast of Iceland and Norway, 11.5 m along the east coast of Greenland, and 18 m and 5.3 m along the north and east coasts of Scotland, respectively. These latter figures agree with field evidence in Scotland showing that the wave reached 4 m above contemporary sea level at most locations in northeastern Scotland, 10 m at the northern tip of Scotland, and 19 m on the Shetland Islands. Along the Norwegian coast, tsunami deposits indicate that run-ups reached 10 m–11 m above sea level along the coastline adjacent to the headwall of the slide, and up to 4 m elsewhere.

The most prominent signature of the Storegga tsunami is the presence of thin sand layers sandwiched between silty clays and buried 3 m–4 m below the surface of the raised estuarine plains or carseland of eastern Scotland (Figure 6.10). These deposits have been described at over 17 sites and are best developed in the Firth of Forth region, where they can be found more than 80 km inland. This long penetration up what was then a shallow estuary is beyond the capacity of even the largest storms in the North Sea and requires tsunami wave amplitudes at the maximum range of those modeled. Generally, the tsunami deposited these sand layers 4 m above the high-tide limit. The presence of these buried sand layers has been known since 1865; however, it wasn't until the late 1980s that researchers realized that the sands were evidence of tsunami originating from the Storegga submarine slides. The basic characteristics of the sands have already been described in Chapter 3. The sands, some of which are gravelly, include marine and brackish diatoms and peat fragments from the underlying sediments. The most common diatom species is *Paralia sulcata* (Ehrenberg) Cleve, which constitutes over 60% of specimens. Many of the diatoms are broken and eroded—features indicative of transport and deposition under high-energy conditions. Generally, the anomalous layer comprises gray, micaceous, silty fine sand less than 10 cm thick, although thicknesses of 75 cm have been found. In places, multiple layers exist, consisting of a series of layers of moderately sorted sand. Grain size fines upward both within individual units and throughout the series. Detailed size analysis indicates that as many as five waves may have reached the coast, with the first and second waves having the greatest energy (Figure 3.4).

This sequence of sands is also well preserved in raised lakes along the Norwegian coast. As the tsunami raced up to 11 m above sea level, it first eroded the seaward portion of coastal lakes around Bjugn and Sula, located adjacent to the headwall of

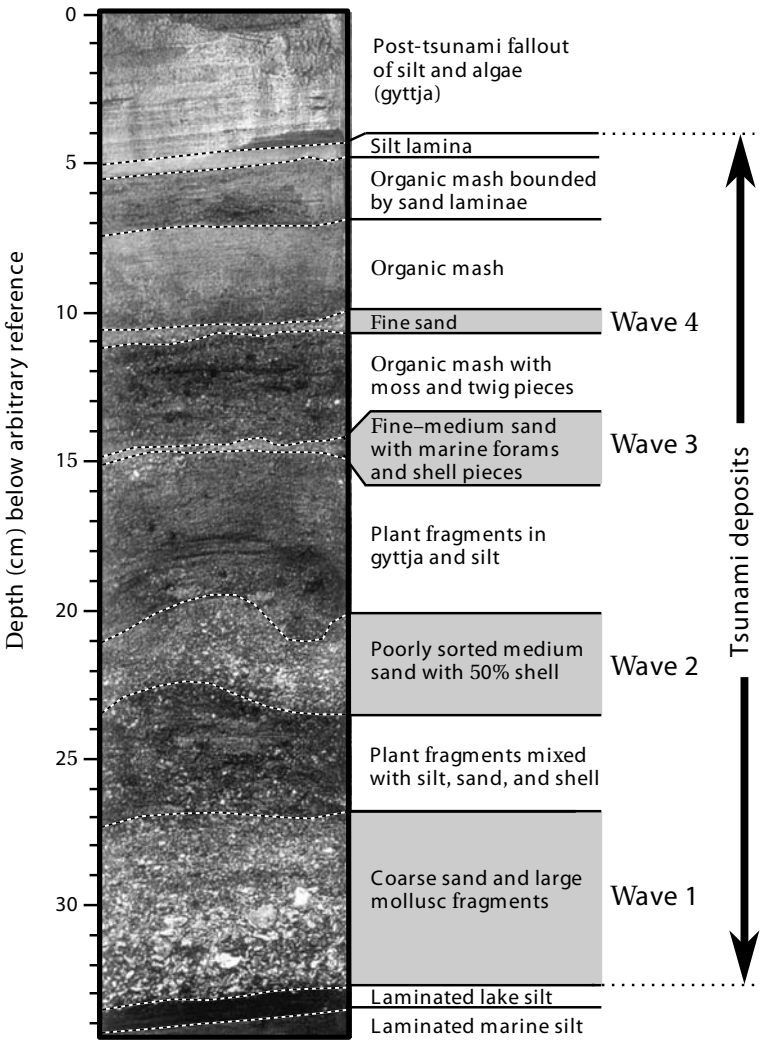

Figure 6.11. Alternating layers of sand and organic debris deposited by four successive tsunami waves of diminishing height in Kvennavatnet lake basin near Bjugn, Norway, following the second Storegga slide. From fig. 6 in Bondevik *et al.* (1997). The photograph is © Blackwell Publishing Ltd. and is reproduced by permission.

the Storegga Slides (Figure 6.10). The wave then laid down a graded or massive sand layer containing marine fossils. As the wave lost energy upslope, it deposited a thinner layer of fining sand. Only one wave penetrated the upper portions of the lakes, but closer to the sea, up to four waves deposited successively thinner layers of sediment in deposits 20 cm–200 cm thick (Figure 6.11). As each wave reached its maximum limit inland, there was a short period of undisturbed flow during which

larger debris such as rip-up clasts, waterlogged wood fragments; and fine sand and organic debris, torn up and mulched by the passage of the tsunami wave, accumulated over the sands. Fish bones from the marine species *Pollachius vierns* (coalfish) and buds from *Alnus* spp. (alder) were found in the organic mash. Both the length of the fish bones and the stage of development of the buds indicate that the event occurred in the late autumn. Each backwash eroded into the freshly deposited organic layer, but because water was ponded in lakes, velocities were not as high as in the run-up. Finally, when the waves abated, fine silt and sand settled from suspension in the turbid lake waters and capped the tsunami deposit with thin, muddy layers of silt termed *gyttja*.

The buried sand is not the only evidence of the Storegga tsunami. The 1 m to 3 m open ocean amplitude of the wave ensured that its effects were widespread throughout the North Atlantic. Besides the buried sands, a raised dump deposit of sand and cobbles has been found at Bitrufjorour, Iceland. Large aligned boulders have also been found along the Skagerrak coast of Sweden pointing toward the slides. Finally, a buried splay of sand, sandwiched between two peat layers, rises to the surface of an infilled embayment on the west coast of Scotland at Mointeach Mohr. The extent and sheltered location of this site rules out storm surge as the mechanism of deposition. The contact between the sand and the older, lower peat unit is erosional, with pieces of the lower peat incorporated into the sand. It appears that the sands in the tsunami deposit originated from the beach and dunes at the mouth of the embayment and were deposited rapidly landward in a similar fashion to the model proposed for tsunami-swept barriers in Chapter 4 (Figure 4.3).

This evidence certainly indicates that the tsunami was large enough to have been very erosive along exposed rocky coasts. Indeed, bedrock-sculptured features and tsunami-generated landscapes of the type described in Chapters 3 and 4, respectively, are present along the east coast of Scotland in the Edinburgh area and prominently along the Grampian coastline north of Aberdeen (Figure 6.10). Ironically, many of these features are similar to those originally described by Hall in his ill-fated hypothesis. For example, a raised fluted rock drumlin is cut into Carboniferous sandstone on the low-tide platform at St. Andrews (Figure 6.12). The crest of the feature lies 2 m above high tide and over 150 m from the backing cliff. Although weathered, the sides of the flute still preserve the distinct form of cavettos, while the upper surface is imprinted with muschelbrüche (scalloped-shaped depressions) aligned parallel to the alignment of features. Transverse troughs, formed by roller vortices, have been carved out from the surrounding platform and are not only aligned with the strike of the sandstone beds, but also perpendicular to the rock drumlin alignment. The platform surface rather than being planed by storm waves has a relief of 0.4 m–0.6 m, dominated by rock plucking that forms smaller flutes aligned parallel to the main feature.

Similar, but more effective, erosion with large-scale development of fluted promontories is most prominent along the Grampian coastline between Fraserburgh and Logie Head. The sand layer deposited by the second Storegga tsunami reaches its maximum thickness—75 cm—along the coast at Fraserburgh. Platforms and promontories have been cut into sandstones and metamorphic slates, phyllites, and

Figure 6.12. Raised rock drumlin or flute on the platform at St. Andrews, Scotland. The rock drumlin preserves sculptured *S*-forms in the form of muschelbrüche and cavettos. Weathering has subsequently modified these features. Roller vortices have cut transverse troughs into the platform surfaces.

schists. One of the better examples of large-scale sculpturing occurs at MacDuff. Here, bedrock has been shaped into large rock drumlins or flutes rising 7 m–8 m above the high-tide line (Figure 6.13). The drumlins are dominated by profuse rock plucking, are detached from each other and the backing cliff, and rise *en echelon* landward, where they end abruptly in a well-developed cliff whose base is slightly raised, about 2 m–3 m above the berm line of the modern beach. While plucking dominates, the sides of some flutes have been carved smoothly and the *en echelon* arrangement is suggestive of helical flow under catastrophic flow. Despite the irregular nature of the eroded bedrock surfaces, smooth potholes appear on the seaward sides of some flutes. These potholes lie above the present active wave zone. In one case, vortex formation on the front and back of a stack has carved out a porthole aligned toward the headwall of the Storegga Slides (Figure 6.13). Similar forms have been linked to tsunami in eastern Australia, where vortices peel off the ends of headlands (Figure 3.25). Farther north, at Gardenstown and Cullen, isolated fluted stacks over 4 m high are present in the middle of embayments (Figure 6.14). The features are so remotely linked to the adjacent rock coastline that in some cases they appear as stranded erosional remnants in the middle of beaches. Their upper parts often lie above the limit of present storm waves. Many flutes still show evidence of cavettos along their sides. The alignment of the flutes is structurally controlled, but the features are best developed where the strike of the bedrock points toward the headwall of the Storegga slides.

Tsunami also have molded headlands. For example, at Logie Head, the end of the headland, which rises over 15 m above present sea level, is separated from the main cliffline by an erosional depression (Figure 6.15). The toothbrush-shaped form is similar to the eroded headlands of southeast Australia interpreted as a prominent signature of tsunami-eroded bedrock terrain (Figures 3.23 and 4.1). Concentrated high-velocity flow or even wave breaking over the back of the headland generates

Figure 6.13. Detached rock drumlins or flutes lying *en echelon* along the coastline at MacDuff, Scotland. Plucking dominates as the main mechanism of erosion, but smooth sculptured features such as potholes and muschelbrüche can be distinguished at a smaller scale. The porthole has formed through vortex formation on the front and back of the stack. The porthole and islet in the middle point towards the headwall of the Storegga slide.

such erosional forms. Large storms can be ruled out as a mechanism for molding these bedrock-sculptured features. Although North Sea storms can generate 15 m high waves superimposed on a 2 m high storm surge, such waves are short in wavelength and break offshore of headlands. Both fluted terrain and the chiseled headland at Logie Head require sustained, high-velocity, unidirectional flow that only a catastrophic tsunami resulting from a mega-slide or asteroid impact into the sea could produce.

It might also be conceivable to attribute such features to glacial activity or to subglacial flow. After all, the features Hall described were later attributed to just such a process. Indeed, the orientation of flutes along the Grampian coastline corresponds to flow lines for the Late Devensian ice sheet that covered this region. However, the fluted features at St. Andrews (and east of Edinburgh at Dunbar), which also point in the same general direction as those along the Grampian coast, are not aligned with the direction of ice sheet movement. Finally, if the flutes are the products of glaciation or catastrophic sub-glacial water flow, then the features should not be limited just to the immediate coastline. Their similarity to features in southeastern Australia, which at no time has been affected by glacial ice during the Pleistocene, implies a common

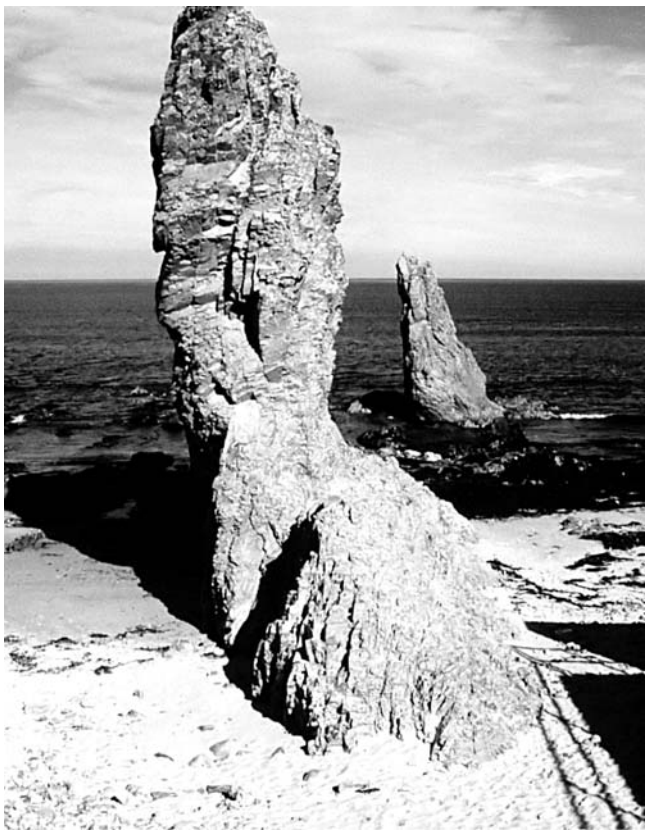

Figure 6.14. Fluted stacks about 4 m high on the beach at Cullen, Scotland. Although weathered, each stack still preserves numerous cavettos on its flanks. The flutes align toward the headwall of the Storegga slide.

mechanism for both localities. It is only fitting that after 150 years, evidence can be found in eastern Scotland for Hall's 1812 hypothesis for bedrock sculpturing by catastrophic tsunami—albeit on a smaller scale than he envisaged.

BRISTOL CHANNEL, U.K., JANUARY 30, 1607

(Anon. 1607, 1762; White, 1607; Mee, 1951; Boon, 1980; Morgan, 1982; Kenyon, 1987; Williams and Davies, 1987; Bryant and Haslett, 2003; Haslett and Bryant, 2005)

In northwestern Europe, the Storegga Slides are not unique. The 1,000 m bathymetric contour is the site of at least 15 other slides on the continental slope between west Ireland and northern Norway. The largest of these is equivalent in size to the smallest Storegga Slide. At least seven of these slides exist along the coast of Ireland within a few hundred kilometers of the coast. Remnant slides also exist on underwater

Figure 6.15. The toothbrush-shaped headland at Logie Head. The larger depression has formed either by catastrophic wave breaking near the shoreline or by concentrated high-velocity flow.

platforms between the British Isles and Iceland with a debris flow, again as large as the smaller Storegga Slide, situated at the base of the Rockall Trough. These slides are undated.

However, one of them may have failed in historical time and affected the Bristol Channel and Severn Estuary on the west coast of the United Kingdom. Historic floods here are reasonably well documented; however, the flood of January 30, 1607 was catastrophic. It flooded 518 km^2 along 570 km of coastline (Figure 6.16), killed up to 2,000 people (Figure 6.1), and resulted in economic loss from which the region never recovered. It was Britain's worst disaster on land. The area affected extended from Barnstaple in Devon and Carmarthen in Wales to the head of the Severn Estuary at Gloucester. Flooding was most severe around Carmarthen, Burnham-on-Sea, Kingston Seymour, and Newport. The greatest death toll appears to be centered on Burnham-on-Sea. At Bridgwater 10 km south of this town, 500 drowned and were buried in a mass grave. Many local churches around Kingston Seymour and Newport record the event with commemorative plaques showing that flood levels were 7.74 m and 7.14 m, respectively, above mean sea level. In the former region, floodwaters 1.5 m deep persisted across the flat marshland for 10 days. Many of the lowlands in the upper reaches of the Channel were protected by levees with sluice gates strategically placed to drain water at low tide after heavy rains. Keepers manned the sluice gates permanently. The 1607 event overtopped the levees and probably drowned these keepers. It then took 10 days for rescuers to get to the gates and open them to release the impounded waters. The maximum flood depth of these entrapped waters was 3.7 m.

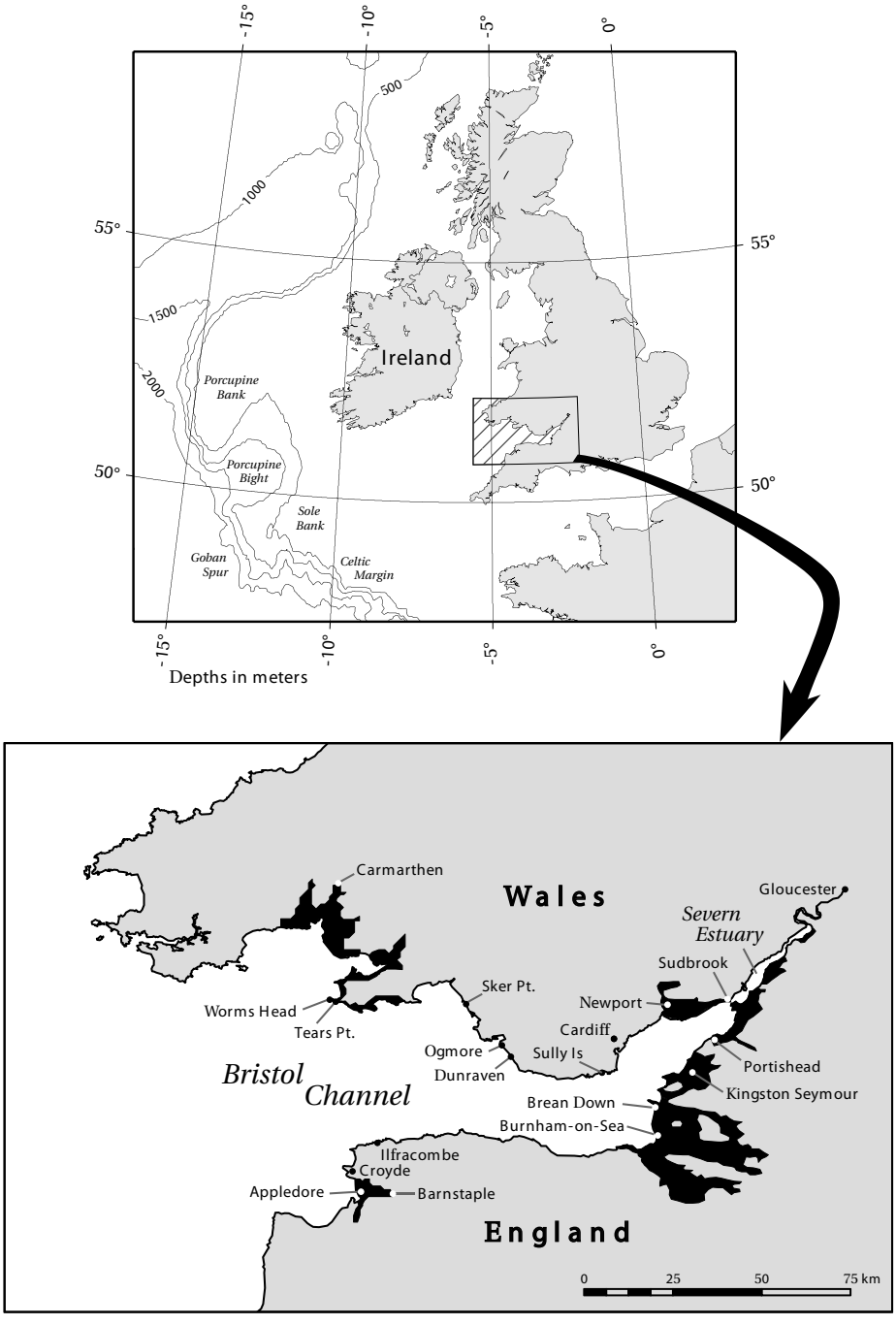

Figure 6.16. Location map of the Bristol Channel, U.K. Black shaded area shows extent of the 1607 flooding.

The flood occurred on a clear day and took residents by surprise. Descriptions of the event have many of the characteristics of recent catastrophic tsunami:

> " ... for about nine of the morning, the same being most fayrely and brightly spred, many of the inhabitants of these countreys prepared themselves to their affayres then they might see and perceive afar off as it were in the element huge and mighty hilles of water tombling over one another in such sort as if the greatest mountains in the world had overwhelmed the lowe villages or marshy grounds. Sometimes it dazzled many of the spectators that they imagined it had bin some fogge or mist coming with great swiftness toward them and with such a smoke as if mountains were all on fire, and to the view of some it seemed as if myriads of thousands of arrows had been shot forth all at one time." (Mee, 1951)

The reference to dazzling, fiery mountains, and myriads of arrows, is similar to accounts of tsunami on the Burin Peninsula, Newfoundland in 1929 where the tsunami crest was shining like car headlights, and in Papua New Guinea in 1998 where the tsunami was frothing and sparkling. In addition the wave approached at great speed:

> " ... affirmed to have runne ... with a swiftness so incredible, as that no gray-hounde could have escaped by running before them." (Morgan, 1882)

Finally, a fully laden 60-tonne ship ready to set sail at Appledore in north Devon was transported from the harbor onto marshland by the wave, a situation that is unlikely if storm conditions were prevailing at the time.

Geomorphic evidence for tsunami in the Channel can be found in the form of transported and imbricated boulders, bedrock sculpturing on coastal platforms and ramps, and, at isolated locations, wholesale erosion of the coastal landscape. Features of bedrock sculpturing are ephemeral, but telling. At Ilfracombe, 30 cm high flutes are cut into slate beds at a low 5° angle aligned with the direction of tsunami approach (Figure 6.17). These smaller flutes are superimposed upon sail-like structures about 5 m high having the same orientation. The flutes give the sails a cockscomb-like appearance similar to those in Figures 3.24 and 4.14 linked to mega-tsunami. At Ogmore, erosion has cut through beds dipping 5° seaward producing a shallow vortex pool with a central plug (Figure 6.18). This feature is similar to those produced along the New South Wales coast by mega-tsunami (Figure 3.21). Hummocky topography representing the presence of a myriad of vortices exists on a ramped surface rising above the level of high tides at Worms Head. Finally, there are indications that tsunami have reshaped some of the rocky coastline in the channel. At Sully Island west of Cardiff, Triassic Red Beds overlie Carboniferous Limestone. Here, a raised platform surface 3 m–4 m above high-tide mark has been eroded with removal of the weaker Red Beds. At Ball Rock, 0.5 km up the channel and sheltered by Sully Island from storm waves, erosion has generated an inverted toothbrush-shaped headland (Figure 6.19) similar to those generated by high-velocity tsunami flow along the New South Wales coast of Australia (Figure 3.23).

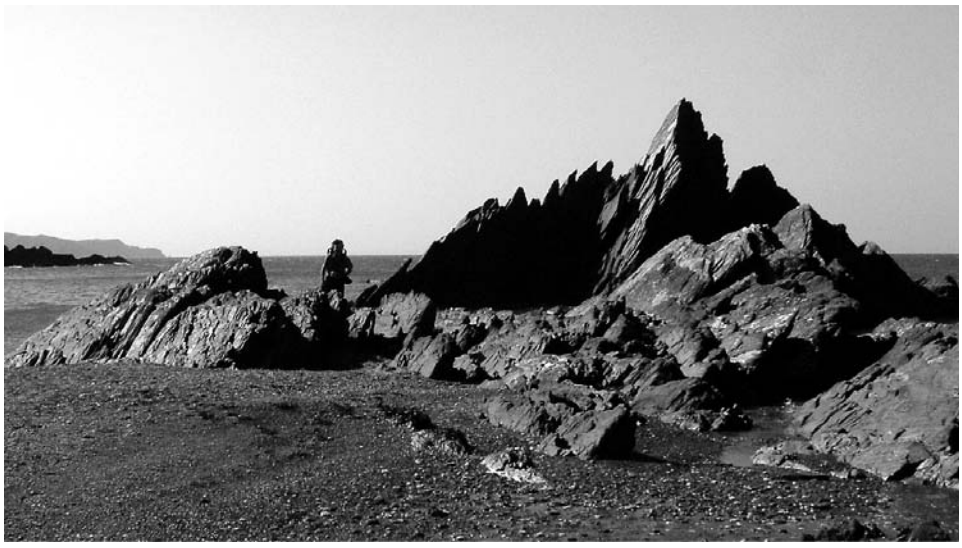

Figure 6.17. Fluting in bedrock at Ifracombe, Devon, U.K.

Figure 6.18. Shallow vortex pool with central plug at Ogmore, South Wales.

Figure 6.19. Inverted toothbrush-shaped promontory at Ball Rock near Sully Island, South Wales.

Also relevant are numerous deposits of boulders around the Channel and Estuary. The characteristics of these boulders and the velocities and wave heights required to move them are summarized in Table 6.2. The latter are calculated using the equations presented in Chapter 3. The largest boulder in the coastal zone is found at Brean Down and weighs 132 tonnes. It requires a tsunami wave only 5.3 m high to move it as opposed to a storm wave 21.3 m high. Because of its flat profile, the boulder with the greatest resistance to flow—found at Tears Point—requires a tsunami height of 8.4 m and a storm wave height of 33.6 m to transport it. The highest storm waves measured in the channel are much less than these heights. The 1 : 50 year wave height is about 10 m at the ocean end of the channel, 4.7 m at sites like Brean Down and Tears Point halfway up the Channel, and 3.5 m at the entrance to the Severn Estuary. In contrast, theoretical tsunami wave heights required to move the boulders increase inland from 4 m at the ocean end to 6 m at the beginning of the Severn Estuary. This increase is inversely proportional to the height of storm waves and the width of the channel—the latter being a result that would be expected as a tsunami traveled up a funnel-shaped channel. Maximum run-up velocities reach 16.2 m s^{-1} at the entrance to the Severn Estuary. These velocities are in the range needed for bedrock sculpturing.

There are other characteristics besides hydrodynamic ones that implicate tsunami as the mode of transport. Table 6.3 catalogs each site according to the ten characteristics of boulder deposits indicative of tsunami transport. Three locations—Dunraven, Tears Point, and Brean Down—have nine of these ten characteristics. The fact that boulders are deposited in groups, have not been flicked into position by storm waves, show signs of lateral transport, and have imbrications that match the approach of the tsunami wave are strong indicators that a tsunami entered the channel and began to move large boulders. One of the best sites showing evidence for a tsunami occurs at Dunraven. Here, the boulders occur in a train, are clearly imbricated against each other, and do not show evidence of percussion at contacts—all features indicative of suspension transport (Figure 6.20). Hydrodynamically, the largest boulder here requires a storm wave of 19.3 m in height,

Table 6.2. Boulder dimensions and inferred flow characteristics at various sites around the Bristol Channel and Severn Estuary, U.K.

Area	*Site*	*A-axis* (m)	*B-axis* (m)	*C-axis* (m)	*Volume* (m^3)	*Weight* (t)	*Velocity of run-up* ($m\,s^{-1}$)	*Distance inland* (km)	*Height of tsunami at shore* (m)	*Breaking storm-wave height* (m)
Severn Estuary	Sudbrook	4.5	3.6	0.7	11.2	25.6	16.2	4.9	6.1	24.4
	Portishead	2.6	2.5	0.2	1.5	3.4	14.9	4.0	5.7	22.7
Inner Bristol Channel	Brean Down	5.2	4.8	2.1	51.4	132.0	14.5	3.7	5.3	21.3
	Sully Island	2.2	1.6	0.3	0.9	2.3	11.8	2.1	3.7	14.9
	Dunraven Bay	2.9	2.8	0.6	5.2	13.3	13.8	3.2	4.8	19.3
	Ogmore	4.9	3.1	1.1	15.8	40.6	13.5	3.1	4.6	18.6
	Sker Point	4.4	4.1	0.9	15.3	41.5	18.1	6.7	8.4	33.6
Outer Bristol Channel	Tears Point	2.1	2.1	0.4	1.8	4.7	12.3	2.4	3.8	15.4
	Croyde	3.0	2.3	0.7	4.5	11.8	12.4	2.5	3.9	15.7

Table 6.3. Proportion of boulders showing tsunami-transport characteristics.

Characteristic of tsunami-transported boulders	*Sites*									
	Sud-brook	*Portis-head*	*Brean Down*	*Sully Island*	*Dun-raven*	*Ogmore*	*Sker Point*	*Tears Point*	*Croyde*	*Number of sites showing charac-teristic (out of 9)*
Deposited in groups	✓	✓	✓	✓	✓	✓	✓	✓	✓	9
Only boulders	✓	✓		✓	✓		✓	✓	✓	7
Imbricated and contact supported				✓	✓		✓	✓		4
Evidence of suspension transport				✓	✓		✓	✓		4
Evidence of lateral transport	✓	✓	✓	✓	✓		✓	✓		7
Above the storm-wave limit		✓					✓	✓	✓	4
Not flicked by storm waves	✓	✓	✓	✓	✓	✓	✓	✓	✓	9
Determinations exclude storms	✓	✓	✓	✓	✓	✓	✓			7
Direction of tsunami approach	✓	✓	✓	✓	✓		✓	✓	✓	8
Other nearby signatures of tsunami				✓	✓	✓		✓		4
Total number of characteristics (out of 10)	*6*	*7*	*5*	*9*	*9*	*4*	*9*	*9*	*5*	

Figure 6.20. Imbricated boulder train at the eastern end of Dunraven Beach, South Wales.

but a tsunami wave only 4.8 m high. In addition, two rock types are mixed together showing that boulders have not simply fallen from the cliffs, but have been moved laterally inland. This site is more intriguing in that isolated boulders, deposited on the adjacent beach through cliff retreat, all begin shoreward of the deposit as if the beach were swept clean of boulders at one point in time commensurate with deposition of the boulder train. Rates of cliff retreat along this coast range from $0.30\,m\,yr^{-1}$–$34\,m\,yr^{-1}$. The coast, in general, retreated 120 m between 1590 and 1990. At Dunraven, the cliff retreated 111 m from the seaward margin of the scattered boulders on the beach. Based on these data, it appears that the cliff in Dunraven Bay was positioned at the current seaward margin of the boulder lag around AD 1634–1672 and that the imbricated boulders in Figure 6.20 were transported by a high-energy event prior to this time, but not earlier than 1590. The 1607 flood event fits within these temporal constraints.

A possible trigger for a tsunami in this region is most likely an earthquake or submarine slide, or a combination of both. An active fault zone, offshore southern Ireland, experienced a 4.5-magnitude earthquake in the 1980s. Indeed, there is at least one historic account of an earth tremor on the morning of January 30, 1607. Alternatively, the steep continental slope offshore Ireland has a number of locations where large slope failures have occurred—such as the Celtic Margin, Goban Spur, Sole Bank, Porcupine Bank, and Porcupine Bight—that could have generated tsunami that could have reached the Bristol Channel at this time. The quest is to map and date these slides.

THE RISK IN THE WORLD'S OCEANS

Other volcanic islands

(Stoddart, 1950; Holcomb and Searle, 1991; Keating, 1998)

Large debris avalanches are now known to be associated with at least two other mid-ocean volcano complexes, La Réunion in the west Indian Ocean and Tristan da Cunha in the South Atlantic Ocean (Figure 6.2). On Réunion, the Grand Brule Slide fans out from the east coast. It consists of four nested submarine landslides that have

reached depths of 0.5 km, 1.1 km, 2.2 km, and 4.4 km below sea level. The Tristan da Cunha complex consists of three volcanoes rising 3,500 m from the seafloor. All three of these islands are bound by near-vertical cliffs 150 m–500 m high. In places, these cliffs form amphitheaters that appear to be the headwalls of former landslides. The largest of these occurs on the northwest side of Tristan da Cunha itself and is associated with a debris avalanche more than 100 m thick, covering an area of about 1,200 km^2 and having an estimated volume of 150 km^3. The slide has been tentatively dated as younger than 100,000 years.

If amphitheater forms in cliffs or a stellate-shape island are the signatures of former landslides, then this process could have removed between 10% and 50% of the exposed portion of most volcanic islands. For example, in the Pacific Ocean such features appear on American and Western Samoa, Tahiti, the Society Chain, and the Marquesas Group (Figure 6.2). On these islands, the highest sea cliffs do not face the prevailing winds or swell but are protected from marine erosion by reefs. On the island of Tutuila in the Samoan Islands and on the islands of the Manua Group up to half of the volcanic complex is missing. On the Samoan Islands, SeaMARC II side-scan sonar reveals profuse slump blocks, chaotic slumps, landslide sheet flows, turbidites, and avalanche debris flows. Landslides have also removed large portions of the upper parts of Guam in the Mariana Islands and of Rarotonga, Mangaia, and Aiutaki in the Cook Islands. As well, the western half of Volcán Ecuador in the Galápagos Islands is missing. In the Atlantic Ocean, the Cape Verde group and the Island of St. Helena also have marked sea cliffs, while in the Caribbean Sea large headwall scars are evident on the westward sides of Dominica, St. Lucia, and St. Vincent Islands in the Lesser Antilles. The Azores Islands are also faceted with amphitheater scars. In the Indian Ocean, large landslides can be inferred from Gough, Marion, Prince Edward, Amsterdam, St. Paul, Bouvetoya, Possession, and Peter I Islands.

Nor do volcanoes have to emerge above sea level to have undergone failure. The seas are pockmarked by numerous atolls, guyots (eroded volcanic islands), and seamounts evincing amphitheater and stellate forms similar to the above. Mass-wasting is one of the major mechanisms reducing high volcanic islands to guyots. Mapping of submerged guyots on the Hawaiian Ridge shows the same density of landslides as present around the main islands. There are approximately a thousand seamounts higher than 1,000 m in the Pacific Ocean. Over 300 of these seamounts lie along the Mariana Island arc in the west Pacific (Figure 6.2). Many seamounts show extensive turbidites on their flanks and have the potential to generate landslides 20 km^3–50 km^3 in size. The perceived view of an uneroded circular or elliptical atoll is also illusionary. For example, on Johnston Atoll in the Line Islands south of Hawaii, one or more major landslides have removed much of the southern margin. Blocks of carbonate up to a kilometer in size have been detected on the adjacent seabed, which in places has been infilled to a depth of 1,500 m. Ninety-five percent of atolls are in fact polygonal in shape, with deep embayments cut into at least one seaward flank. If the aprons around these features are signs of past landslides, then such deposits cover 10% of the ocean. Whenever there has been a failure, there has been the potential for a tsunami.

Other topography

(Moore, 1978; Kenyon, 1987; Lipman *et al.*, 1988; Carlson, Karl, and Edwards, 1991; Canals *et al.*, 2004)

Other topography besides volcanoes can also produce submarine landslides. These include river deltas, passive continental margins, submarine canyons, deep-sea fans, the walls of deep trenches near subduction zones, and the slopes of mid-ocean ridges. Some of the sites where slides have been identified as originating from these types of topography are mapped in Figure 6.2. Major river deltas are prone to landslides because of the volume of sediment continually being built up on their submerged distal ends. The rivers with the largest sediment loads—the Amazon, Mississippi, Nile, and Indus—have built up relatively steep fans more than 10 km thick. The Amazon Fan consists of several major slide deposits, the largest of which covers an area of 32,000 km^2. Two debris flows have been mapped in 1,000 m–3,000 m depth of water off the Mississippi Delta. The larger of the two is 100 km wide and 300 km long.

Passive continental margins lie along tectonically inactive edges of crustal plates. Many of the slides emanating from these margins are derived from sedimentary units that are only 10 m–100 m thick. Sediment has accumulated over time along these margins through sub-aerial erosion. Failure occurs on slopes parallel to bedding planes. While the size of these slides is small compared with the Hawaiian ones, the widespread nature of the evidence is worrisome. For example, the eastern seaboard of the United States has at least four large submarine canyons cutting through the shelf edge, leading to distributary fans on the abyssal plain. Levees on the fans indicate that large debris or gravity flows have occurred often. Slides are numerous off the west coast of Africa, where hummocky slides, block fields, debris flows, and turbidity deposits have all been mapped. Few submarine slides have yet been detected off the west coast of North America, mainly because bathymetry has not been mapped in detail. However, a 6.8 km^2 slide with a volume of 1 km^3 occurred on April 27, 1975 off the fjord delta at Kitimat, British Columbia. The resulting tsunami had a run-up height of 8.2 m. A 75 km long slide also has been detected off the Monterey Fan in California. One area that has been mapped well is the continental slope on the north side of the Aleutian Islands facing the Bering Sea. The area is relatively quiet seismically but is underlain by gas hydrates or a zone of sedimentary weakness. Here, mass failures up to 55 km long and containing blocks 1 km–2 km across have been identified emanating from some of the largest canyons in the world on low slopes of 0.5°–1.8°. The volume of the landslides ranges between 20 km^3 and 195 km^3.

The sides of deep ocean trenches are only susceptible to submarine slides if ocean sediment has accumulated here as part of a tectonic process. Thick sediment layers can pile up on oversteepened slopes as the result of tectonic off-scraping. Slides from trenches have been reported in the Sunda, Peru–Chile, Puerto Rican, and eastern and western Aleutian Trenches. One of the largest slides occurs in the Sunda Trench off the Bassein River in Burma. The slide covers an area of 3,940 km^2 and has a volume of 960 km^3. The slide was triggered either by an earthquake or by overloading of sediments brought down the Irrawaddi River at lower sea levels. Along other

trenches, localized slides of 10 km length appear to be a common feature. Where crustal plates are sliding past each other, slides can develop in subduction zones. The Ranger slide off the coast of California is one of the biggest of this type identified to date. It covers an area of $125\,km^2$ and incorporates $12\,km^3$ of material. Even mid-ocean ridges can generate slides. Along the Mid-Atlantic Ridge, one such slide, comprising $19\,km^3$ of material, was caused by the failure of a $4\,km \times 5\,km$ block on the flank of a mountain bordering the rift.

More worrisome are the coasts where no mapping has been carried out. Most of the coastline surrounding the Indian Ocean has not been mapped in enough detail to identify individual slides. Even in a developed country such as Australia, parts of the east coast have only been mapped since 1990 using side-scan sonar. This coastline is passive and assumed to have low seismicity. However, a slide measuring $10\,km \times 20\,km$ was detected 50 km off the coast south of Sydney. The age of the slide is unknown, but there is now substantial evidence for the presence of recent large tsunami along the adjacent coastline. As described in Chapter 4, the signatures of tsunami are common elsewhere around Australia, but unfortunately any link to submarine slides remains speculative without detailed mapping.